Electronic Supplementary Material (ESI) for Journal of Materials Chemistry C.

Supporting Information

Application of Indacenodiselenophene Central Core and Modulation of Terminal Group Interaction for High-Efficient P3HT-based Organic Solar Cells

Mengzhen Du[a,b], Yuzhang Xiao[a,b], Yanfang Geng[b], You Chen[b], Hai Jiang[a,b], Chuanqi Dong[a,b], Qiang Guo[a], Qing Guo[a], Gongqiang Li[c], Erjun Zhou[a]**

[a] School of Materials Science and Engineering, Henan Institute of Advanced Technology, Zhengzhou University, Zhengzhou, 450001, China

[b] CAS Key Laboratory of Nanosystem and Hierarchical Fabrication, CAS Center for Excellence in Nanoscience, National Center for Nanoscience and Technology, Beijing, 100190, China

[c] Key Laboratory of Flexible Electronic (KLOFE) & Institute of Advanced Materials (IAM), Nanjing Tech University, 30 South Puzhu Road, Nanjing, 211816, China

E-mail: gengyf@nanoctr.cn; zhouej@nanoctr.cn

1. Synthesis and Characterizations

^{1}H NMR and ^{13}C NMR were measured by using a Bruker Advance III 400 (400 MHz) nuclear magnetic resonance (NMR) spectroscope. MALDI-TOF were obtained using a Bruker Autoflex MAX. UV-vis absorption spectra were obtained on Cary 5000 UV-Vis-NIR (Agilent Technology). Cyclic voltammetry (CV) was tested on an electrochemical workstation with working electrode Pt plate, counter electrode Pt wire and standard calomel electrode (SCE) as reference electrode. The CV curves were recorded versus the potential of SCE, which was calibrated by the ferrocene-ferrocenium (Fc/Fc^{+}) redox couple, whose absolute energy level is 4.8 eV below vacuum.

Scheme S1. Synthetic route of **BTA46** and **BTA47**.

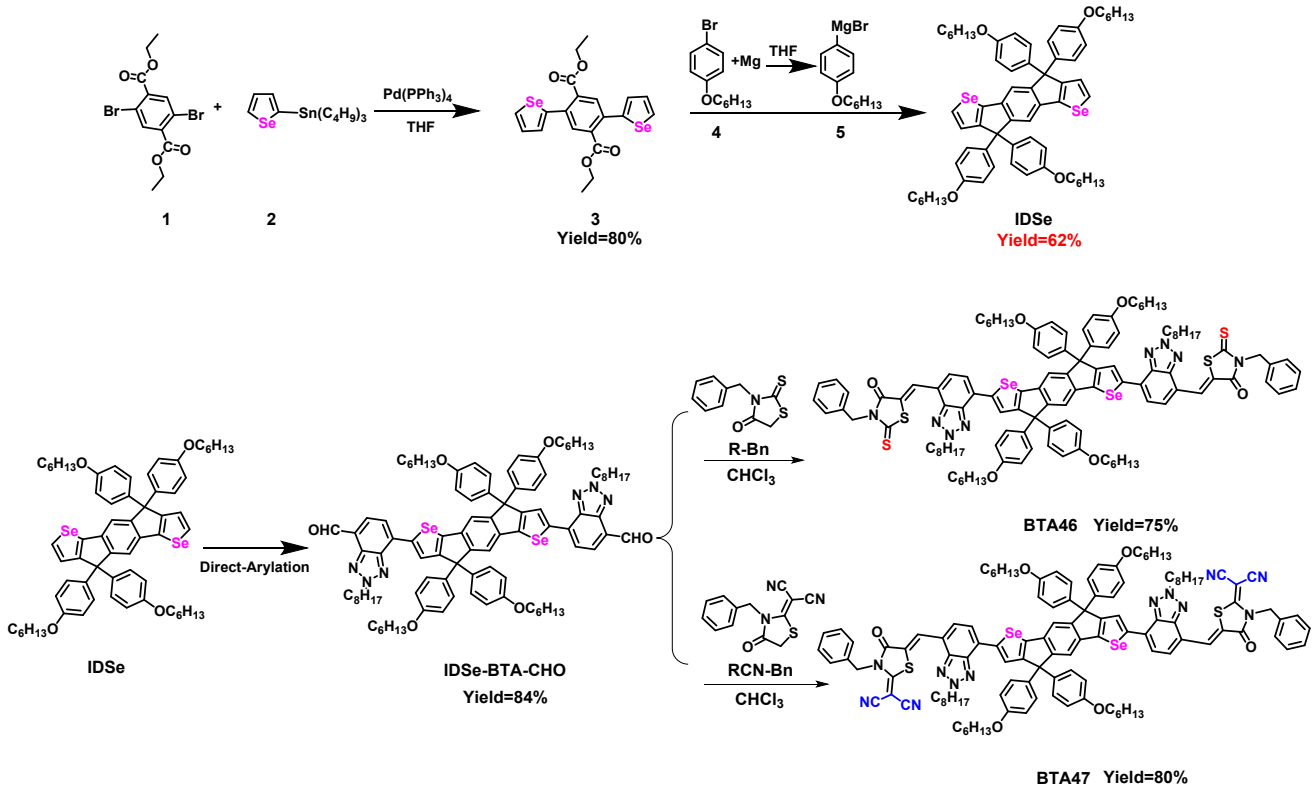

(1) Synthesis of compound 3

To a 50 mL round-bottomed flask was added compound **1** (410 mg, 1.08 mmol), compound **2** (1.0 g, 2.37 mmol), Pd $(PPh_3)_4$ (62.4 mg, 0.05 mmol), and degassed THF (20 mL). The mixture was heated to reflux under N_2 atmosphere for 16 h. Potassium fluoride saturated solution (30 mL) was added and stirred for 6 hours. The mixture was extracted with dichloromethane (3 × 100 mL). The organic phase

was dried over anhydrous magnesium sulfate. After filtration, the solvent was removed under reduced pressure. The residue was purified by column chromatography on silica gel petroleum ether/dichloromethane (1:1), to give compound **3** as a white solid (410 mg, 80%). ^{1}H NMR (400 MHz, Chloroform-d) δ (ppm) 8.08 (d, J = 5.6 Hz, 2H), 7.78 (s, 2H), 7.30 (dd, J = 5.7, 3.8 Hz, 2H), 7.22 (d, J = 3.7 Hz, 2H), 4.21 (q, J = 7.1 Hz, 4H), 1.15 (t, J = 7.1 Hz, 6H).

(2) Synthesis of IDSe

1 mol/L Grignard reagent was prepared according to the following procedure. Added magnesium chips (535 mg, 22.0 mmol) and half of iodine in a dry 100 mL two-necked vial. Under a N_2 atmosphere, 20 mL of now-steamed THF is taken with a syringe and injected into the two-necked flask. Turn on the stirring, at first add 2-3 drops of 1-bromo-4-(hexyloxy) benzene into the bottle, and blow the system to a slight boil with a hair dryer, the system immediately changes from yellow to colorless and gradually turns gray, indicating that the reaction has been initiated, then slowly add the remaining 1-bromo-4-(hexyloxy) benzene drop by drop. Transfer to an oil-bath pans and reflux for 1.5 hours after the system has stabilized, turn off the heating and stirring and return to room temperature. Another dry 100mL two-mouth flask was added with compound **3** (410 mg, 0.85 mmol) and 20 mL of THF, under N_2 atmosphere, the system was slowly added dropwise at room temperature with the 6.8 mL of existing Grignard reagent, and the system slowly changed from yellow to orange-red and gradually burgundy, and refluxed on an oil bath for 16 h. The mixture was extracted with dichloromethane (3 × 100 mL). The organic phase was dried over anhydrous magnesium sulfate. After filtration, the solvent was removed under reduced pressure. The residue was purified by column chromatography on silica gel petroleum ether/dichloromethane (5:1), to give compound **IDSe** as a yellow solid (560 mg, 62%) without the subsequent addition of concentrated sulfuric acid to close the ring. ^{1}H NMR (400 MHz, Chloroform-d) δ (ppm) 7.87 (d, J = 5.4 Hz, 2H), 7.35 (s, 2H), 7.16 (dd, J = 12.6, 6.8 Hz, 10H), 6.76 (d, J = 8.4 Hz, 8H), 3.90 (t, J = 6.6 Hz, 8H), 1.79 – 1.69 (m, 8H), 1.47 – 1.38 (m, 8H), 1.35 – 1.26 (m, 16H), 0.92 – 0.85 (m, 12H). IDSe (MALDI-TOF): m/z calcd for $C_{64}H_{74}O_4Se_2$: 1066.39. Found: 1062.44 [M-4], 1064.45 [M-2], 1066.46 [M].

(3) Synthesis of IDSe-BTA-CHO

To a 10 mL round-bottomed flask was added IDSe (319 mg, 0.3 mmol), 7-bromo-2-octylbenzotriazole-4-carbaldehyde (213 mg, 0.63 mmol), $Pd_2(dba)_3$ (14 mg, 0.015 mmol), tris(2-

methoxyphenyl)phosphine ((o-MeOPh)$_3$P, 11 mg, 0.03 mmol), potassium carbonate (K_2CO_3, 166 mg, 1.2 mmol), pivalic acid (PivOH, 15 mg, 0.15 mmol), and 1,2-dimethylbenzene (ODMB, 1.5 mL). The mixture was heated to 100 °C under N_2 atmosphere for 24 hours. After being cooled to room temperature, the reaction mixture was diluted with chloroform and then filtered to remove the insoluble species. The residue was purified by column chromatography on silica gel petroleum ether/dichloromethane (1:1), to give compound **IDSe-BTA-CHO** as a dark purple solid (400 mg, 84%). ^{1}H NMR (400 MHz, Chloroform-d) δ (ppm) 10.38 (s, 2H), 8.15 (s, 2H), 7.93 (d, J = 7.6 Hz, 2H), 7.74 (d, J = 7.6 Hz, 2H), 7.52 (s, 2H), 7.28 (s, 8H), 6.83 (d, J = 9.0 Hz, 8H), 4.85 (t, J = 7.4 Hz, 4H), 3.91 (t, J = 6.5 Hz, 8H), 2.22 – 2.14 (m, 4H), 1.75 (p, J = 6.6 Hz, 8H), 1.42 (q, J = 6.6, 6.0 Hz, 16H), 1.30 (dp, J = 7.0, 3.1 Hz, 28H), 0.90 – 0.83 (m, 18H).

(4) Synthesis of two NFAs

IDSe-BTA-CHO (158 mg, 0.1 mmol) and end groups (0.3 mmol) were dissolved in chloroform (10 mL). After purged with nitrogen, piperidine (5 drops) was added to the solution. The reaction mixture was stirred at 50 °C. After completion of the reaction (monitored by TLC), 100 mL methanol was added to the resultant mixture, then filtered. The residue was purified by column chromatography on silica gel with chloroform as an eluent yielding a dark solid.

BTA46 (150 mg, 75%). ^{1}H NMR (400 MHz, Chloroform-d) δ (ppm) 8.24 (s, 2H), 8.11 (s, 2H), 7.65 (d, J = 7.8 Hz, 2H), 7.48 (d, J = 6.7 Hz, 4H), 7.46 – 7.42 (m, 4H), 7.35 – 7.27 (m, 6H), 7.26 – 7.22 (m, 8H), 6.82 (d, J = 8.8 Hz, 8H), 5.33 (s, 4H), 4.78 (t, J = 7.1 Hz, 4H), 3.91 (t, J = 6.5 Hz, 8H), 2.22 – 2.14 (m, 4H), 1.74 (p, J = 6.6 Hz, 8H), 1.45 – 1.37 (m, 16H), 1.28 (m, 28H), 0.87 (t, J = 7.7 Hz, 18H).^{13}C NMR (101 MHz, Chloroform-d) δ (ppm) 194.02, 159.27, 158.30, 148.38, 146.23, 136.30, 135.12, 128.68, 128.19, 125.56, 122.08, 121.48, 118.01, 68.07, 63.68, 57.22, 47.70, 31.89, 31.71, 30.04, 29.40, 29.14, 26.69, 25.89, 22.73, 14.17, 1.16. HRMS (MALDI-TOF): m/z calcd for $C_{114}H_{126}N_8O_6S_4Se_2$: 1990.70. Found: 1987.42 [M-3], 1990.75 [M], 1994.47 [M+4].

BTA47 (164 mg, 80%). ^{1}H NMR (400 MHz, Chloroform-d) δ (ppm) 8.36 (s, 2H), 8.16 (s, 2H), 7.69 (d, J = 7.8 Hz, 2H), 7.55 (d, J = 8.1 Hz, 2H), 7.47 (s, 2H), 7.37 (dt, J = 12.3, 6.8 Hz, 6H), 7.29 (d, J = 7.1 Hz, 4H), 7.27 – 7.24 (m, 8H), 6.83 (d, J = 8.9 Hz, 8H), 5.51 (s, 4H), 4.87 – 4.76 (m, 4H), 3.92 (t, J = 6.5 Hz, 8H), 2.22 (q, J = 6.6 Hz, 4H), 1.75 (p, J = 6.6 Hz, 8H), 1.46 – 1.36 (m, 16H), 1.34 – 1.29 (m, 28H), 0.87 (dt, J = 13.2, 6.9 Hz, 18H). ^{13}C NMR (101 MHz, Chloroform-d) δ (ppm) 166.84, 158.36,

136.17, 133.63, 133.01, 131.48, 129.24, 128.63, 127.17, 126.15, 121.46, 118.16, 116.95, 114.47, 113.30, 68.09, 63.71, 57.42, 47.78, 31.86, 31.71, 29.89, 29.40, 29.22, 29.05, 26.68, 25.89, 22.74, 14.17. HRMS (MALDI-TOF): m/z calcd for $C_{120}H_{126}N_{12}O_6S_2Se_2$: 2055.77. Found: 2053.88 [M-2] 2050.93 [M-5], 2055.94 [M].

2. Fabrication and Characterization of Photovoltaic Device

Organic photovoltaic (OPV) device were fabricated with the typical stack-up structure of ITO/PEDOT:PSS/Active Layer/Ca/Al. The indium tin oxide (ITO) glass was cleaned by sequential ultrasonication in detergent, deionized water and anhydrous ethanol for 20 min twice. After drying, the substrates were treated in an ultraviolet-ozone chamber for 15 min. A thin layer of poly (3,4-ethylenedioxythiophene): poly(styrene sulfonate) (PEDOT:PSS) was spin-coated onto the ITO glass as anode interlayer and annealed at 150 °C for 10 min. The substrates were transferred into a glove-box with nitrogen atmosphere. Thin films of active layer were spin-coated from a solution of P3HT:**BTA46** and P3HT:**BTA47** in chloroform at a concentration of 15 and 18mg·mL^{-1}, respectively. The calcium layer (20 nm) and the aluminum layer (100 nm) were then evaporated onto the surface of the active layer under high vacuum as negative electrode. The active area of the device was 4 mm^2.

The *J-V* curve was measured using a Zolix SolarIV-150A-ZZU system. The photocurrent was measured under AM 1.5 G illumination at 100 mW·cm^{-2} using a Zolix HPS-300XA solar simulator. Light intensity is calibrated with a Zolix QE-B1 Si-based solar cell. The EQE spectrum was measured using Zolix SCS10-X150-DSSC-ZZU system.

Hole-only and electron-only devices were fabricated by using the device structures of glass/ITO/PEDOT:PSS/Active Layer/MoO_3/Al and glass ITO/ZnO/Active Layer/Ca/Al, respectively. The active layers were spin-coated from chloroform solution with the total concentration of 15 and 18 mg·mL^{-1}, respectively. Both hole and electron mobilities were calculated using the Mott–Gurney equation: [1]

$$J = \frac{9}{8}\varepsilon_0\varepsilon_r\mu\frac{V^2}{L^3}$$

where J stands for current density, ε_0 is the permittivity of free space (8.85×10^{-12} C·V^{-1}·m^{-1}), ε_r is the relative dielectric constant of the transport medium (assuming that of 3.0), μ is the carrier mobility, V is the internal potential in the device and L is the thickness of the active layer.

3. Measurements

Active thickness: The thickness of the active layer was measured on a Kla-TencorAlpha-StepD-120 Stylus Profiler.

TA spectroscopy: TA spectroscopy was tested by a regenerative amplified Ti:sapphire laser system (Coherent) as the laser source and EOS spectrometer (Ultrafast Systems LLC) as the spectrometer, pump beam excitation intensity at 10 μJ cm^{-2}. In order to separately follow the time evolution of the different exciton and charge contributions, the TA spectra at selected delays were decomposed into a linear combination of three components: donor excitons, acceptor excitons and photogenerated charges. The singlet exciton spectrum of P3HT was taken from the TA spectrum at 1 ps, and the singlet exciton spectrum of BTA46 or BTA47 was extracted from the TA spectrum of the neat acceptor film at 1 ps. The charge signature for all blend films was extracted from the TA data at 1 ns.

GIWAXS Two-dimensional grazing incidence wide angle X-ray scattering (2D-GIWAXS) analyses were measured at the XEUSS SAXS/WAXS equipment. The data were obtained with an area Pilatus 100k detector with a resolution of 195 × 487 pixels (0.172 mm × 0.172 mm). The X-ray wavelength was 1.54 Å, and the incidence angle was 0.2°. The samples were spin-coated onto the PEDOT:PSS/Si substrate.

AFM characterization The AFM height and phase images of blend films were obtained on a Multimode Digital Instrument (D3100) in ScanAsyst mode.

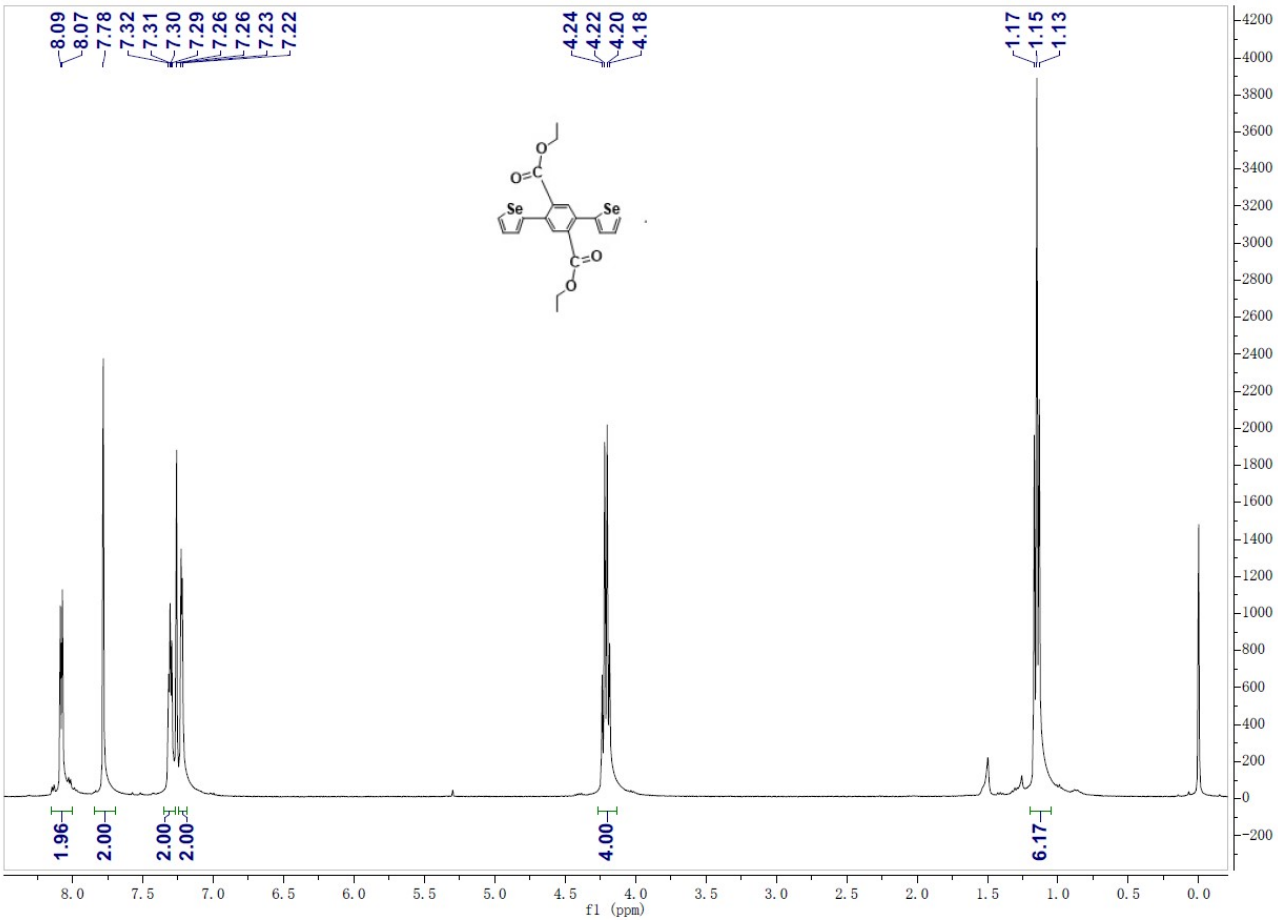

Figure S1. The ^{1}H NMR of compound **3**.

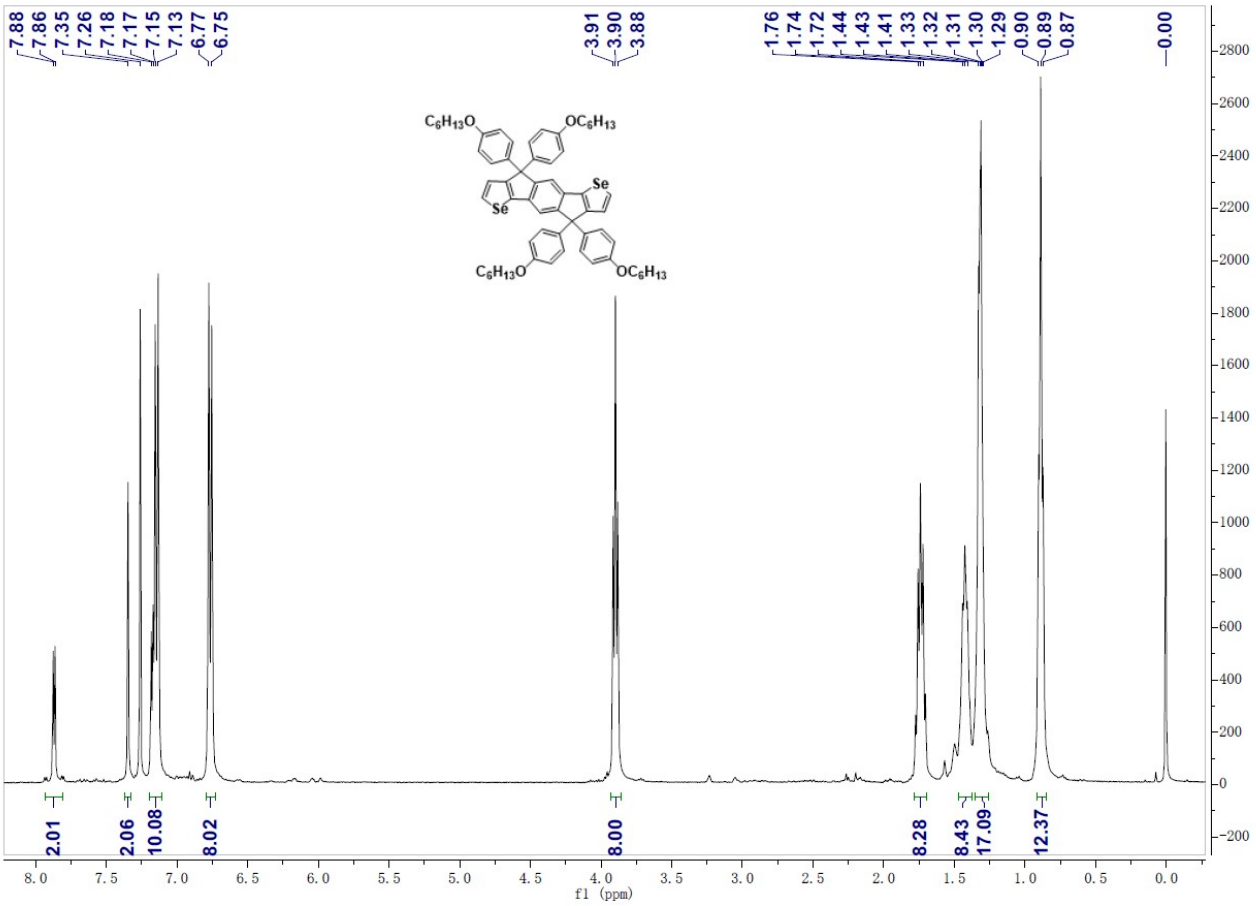

Figure S2. The ^{1}H NMR of **IDSe**.

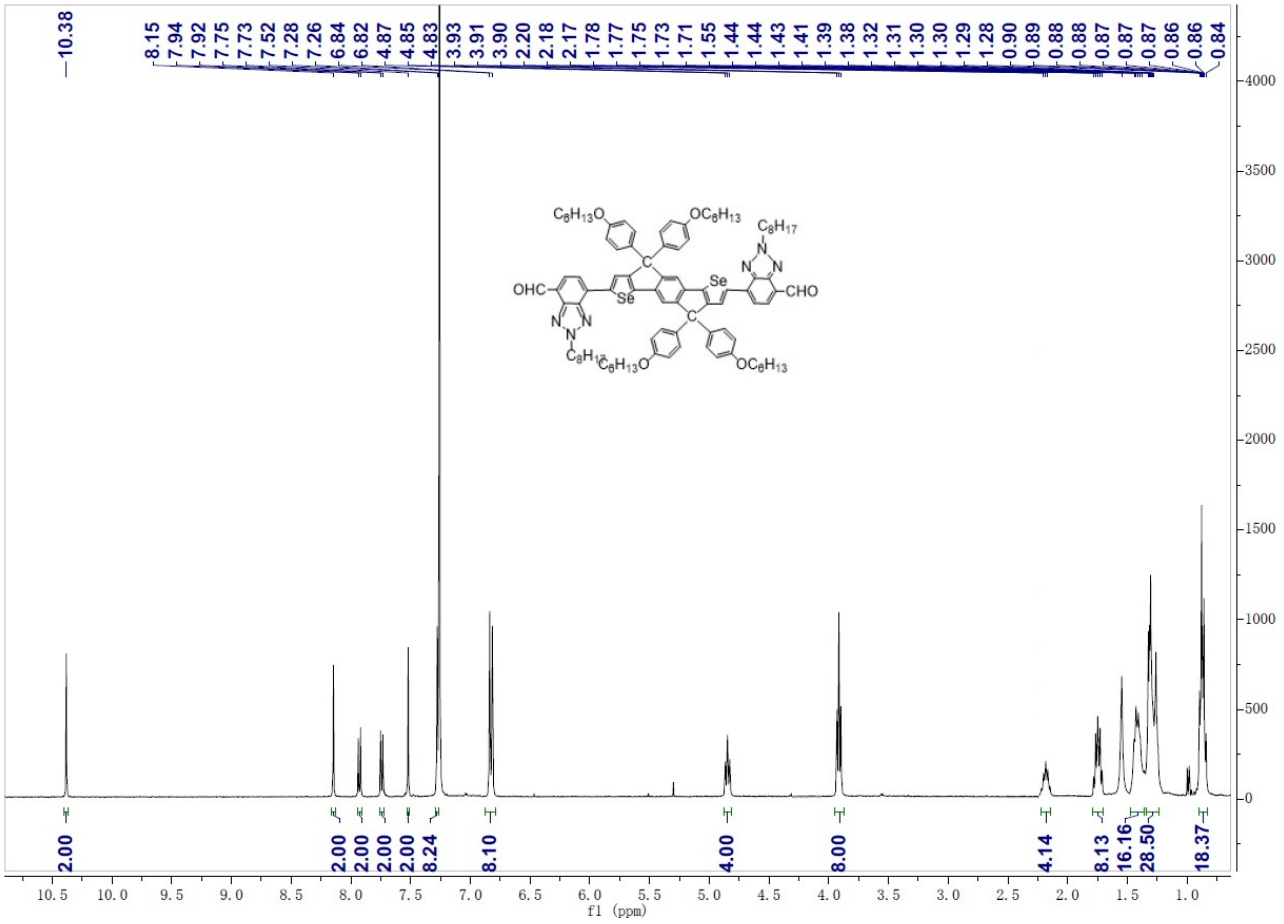

Figure S3. The ^{1}H NMR of IDSe-BTA-CHO.

Figure S4. The ^{1}H NMR of **BTA46**.

Figure S5. The ^{13}C NMR of **BTA46**.

Figure S6. The ^{1}H NMR of **BTA47**.

Figure S7. The ^{13}C NMR of **BTA47**.

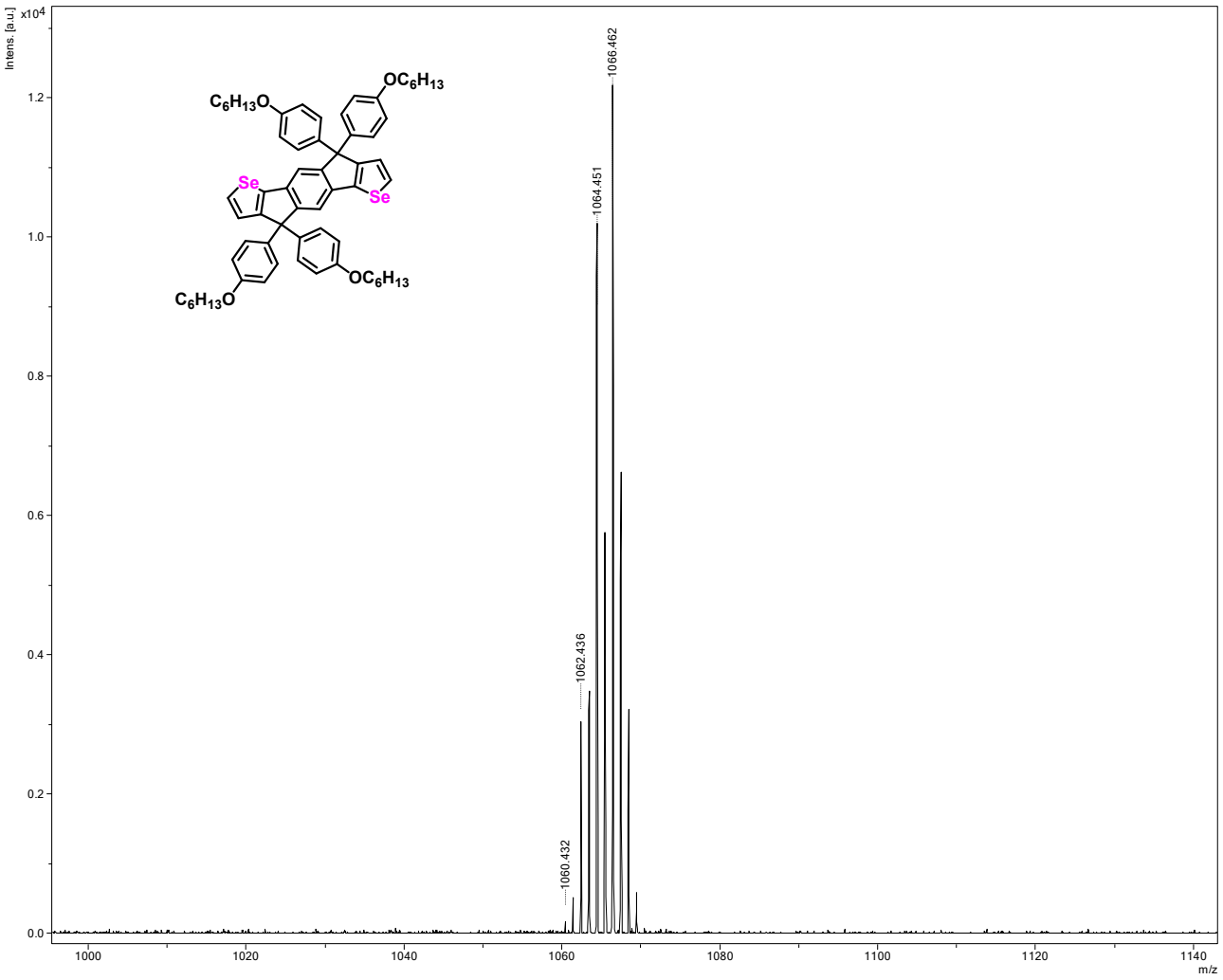

Figure S8. The Mass spectrum of **IDSe**.

Figure S9. The Mass spectrum of **BTA46**.

Figure S10. The Mass spectrum of **BTA47**.

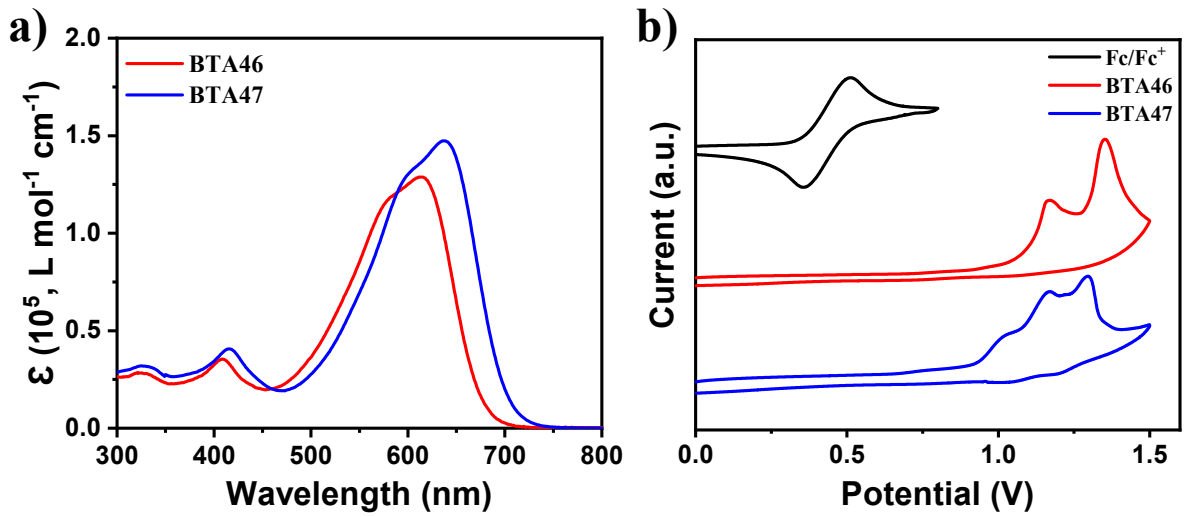

Figure S11. a) UV-vis absorption spectra of **BTA46** and **BTA47** in CF solution (absorption coefficient); and b) Cyclic voltammograms (CV) of **BTA46** and **BTA47** with Ag/AgCl as a reference electrode.

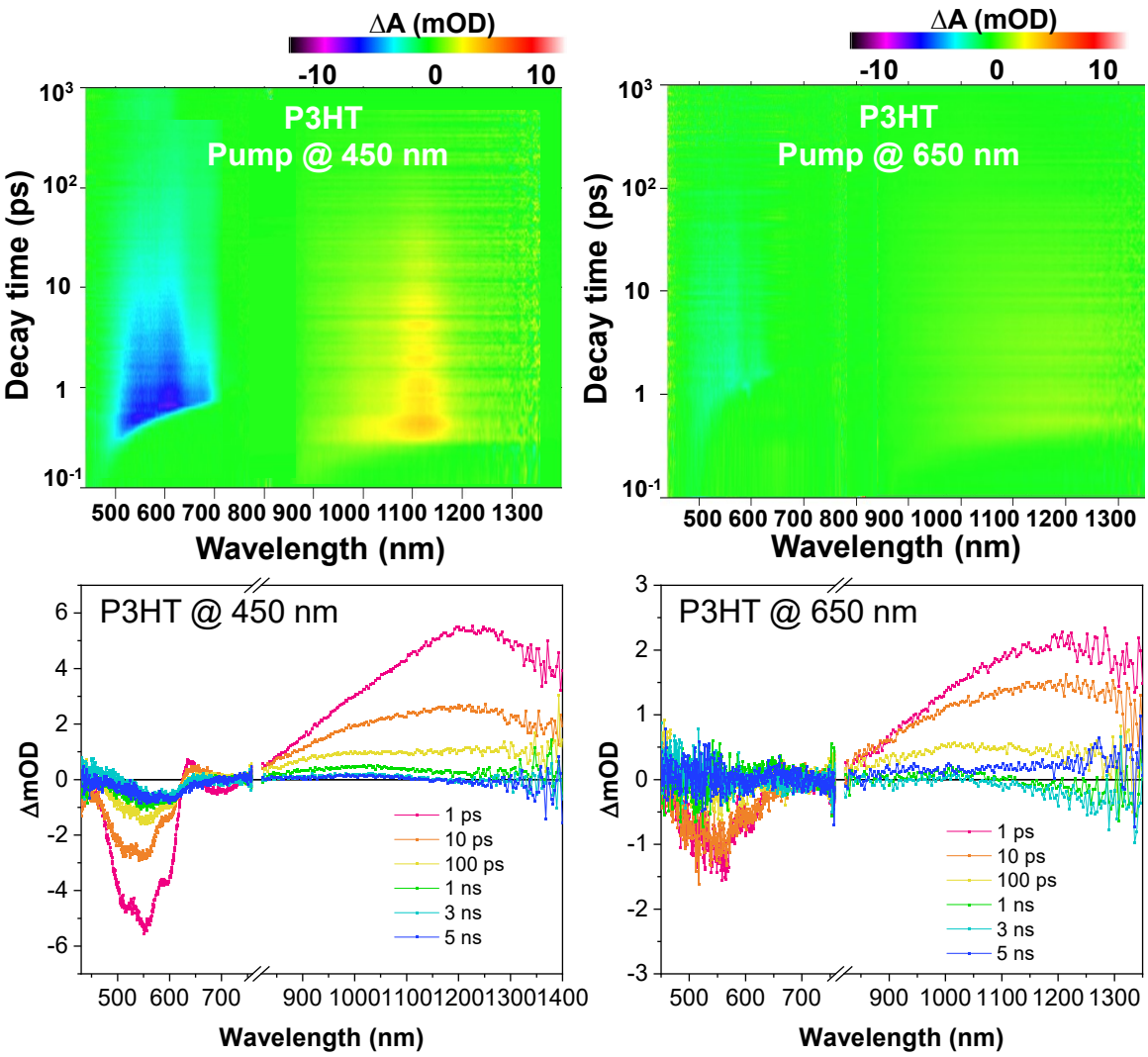

Figure S12. The TA images and the corresponding spectra of **P3HT** neat films measured at 1 ps, 10 ps, 100 ps, 1 ns, 3 ns, and 5 ns after 450 nm and 650 nm laser excitation.

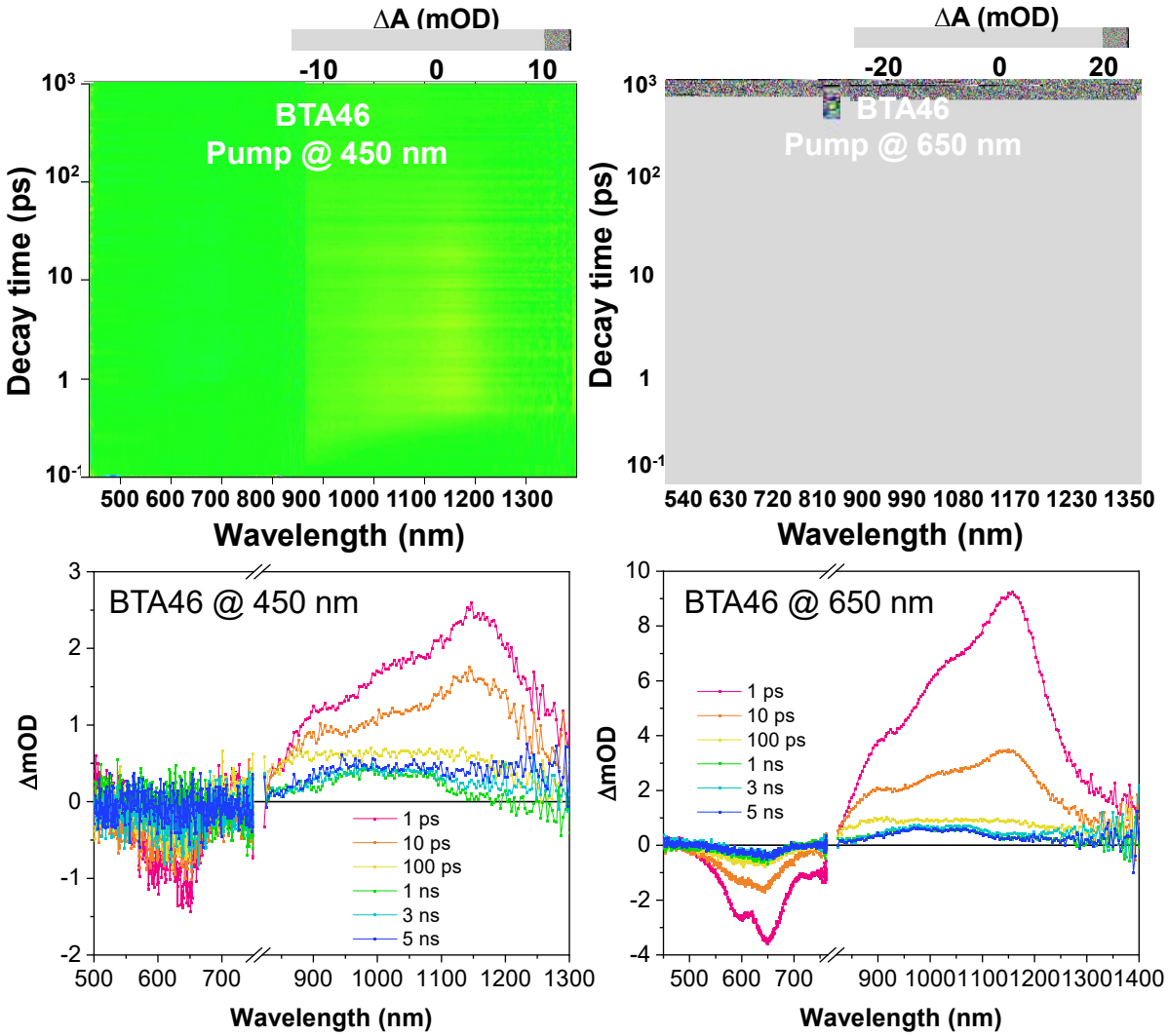

Figure S13. The TA images and the corresponding spectra of **BTA46** neat films measured at 1 ps, 10 ps, 100 ps, 1 ns, 3 ns, and 5 ns after 450 nm and 650 nm laser excitation.

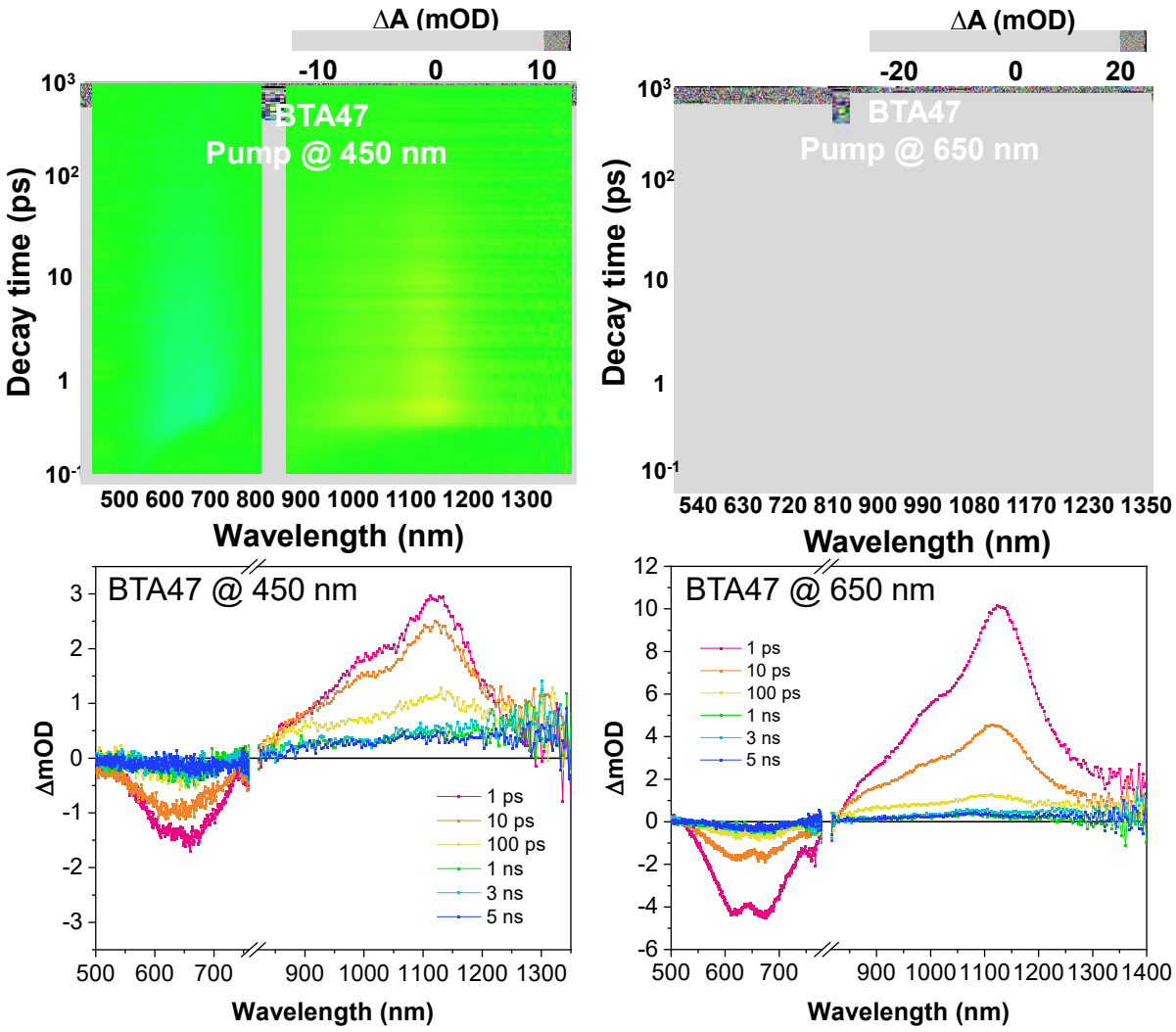

Figure S14. The TA images and the corresponding spectra of **BTA47** neat films measured at 1 ps, 10 ps, 100 ps, 1 ns, 3 ns, and 5 ns after 450 nm and 650 nm laser excitation.

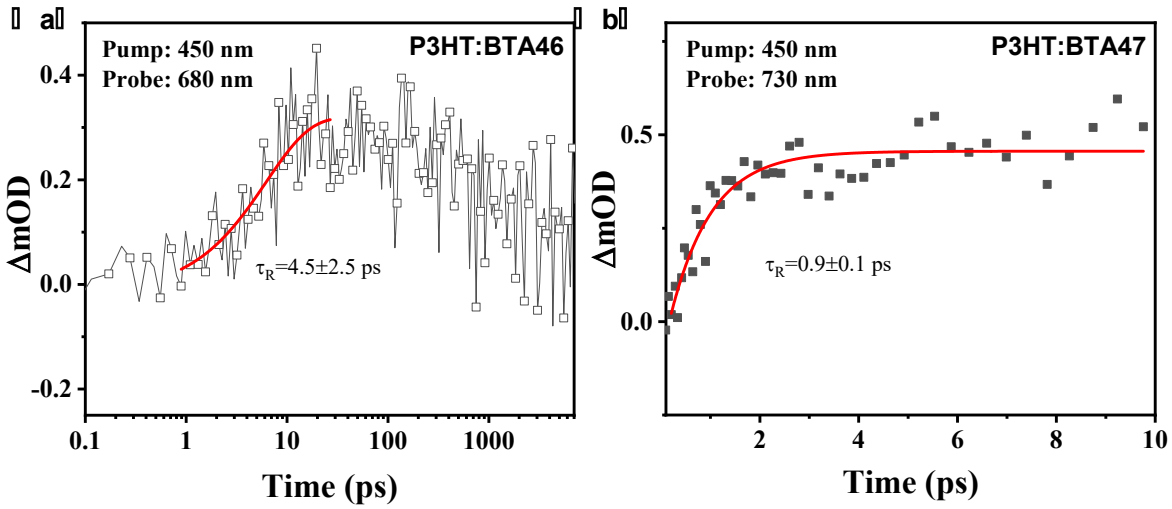

Figure S15. Dynamic fitting of P3HT:**BTA46** and P3HT:**BTA47** blend films excited at 450 nm and 650 nm.

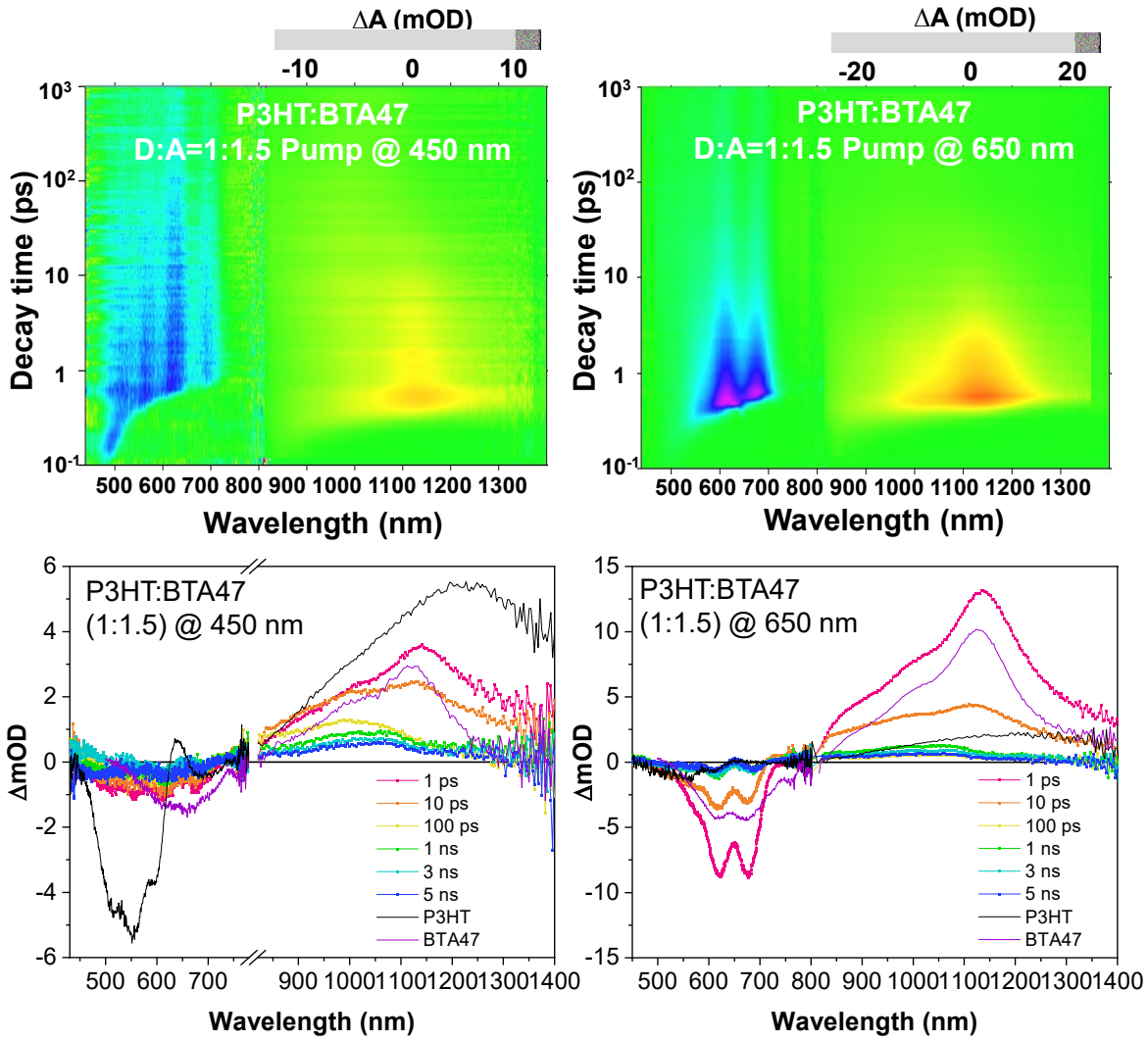

Figure S16. TA images and the corresponding spectra of P3HT:**BTA47** blend films with weight ratio of 1:1.5 measured at 1 ps, 10 ps, 100 ps, 1 ns, 3 ns, and 5 ns after 450 nm and 650 nm laser excitation.

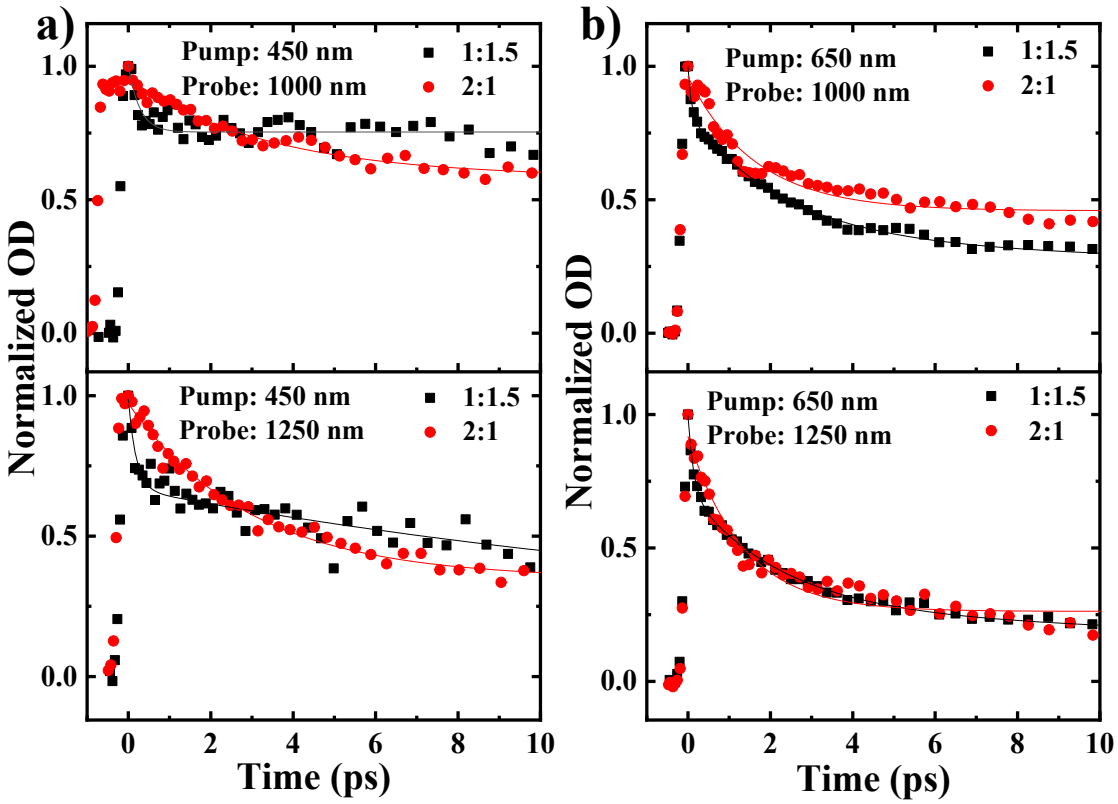

Figure S17. TA signals of P3HT:**BTA47** blend films with D:A weight ratioa of 1:1.5 and optimal 2:1 excited at 450 nm and 650 nm.

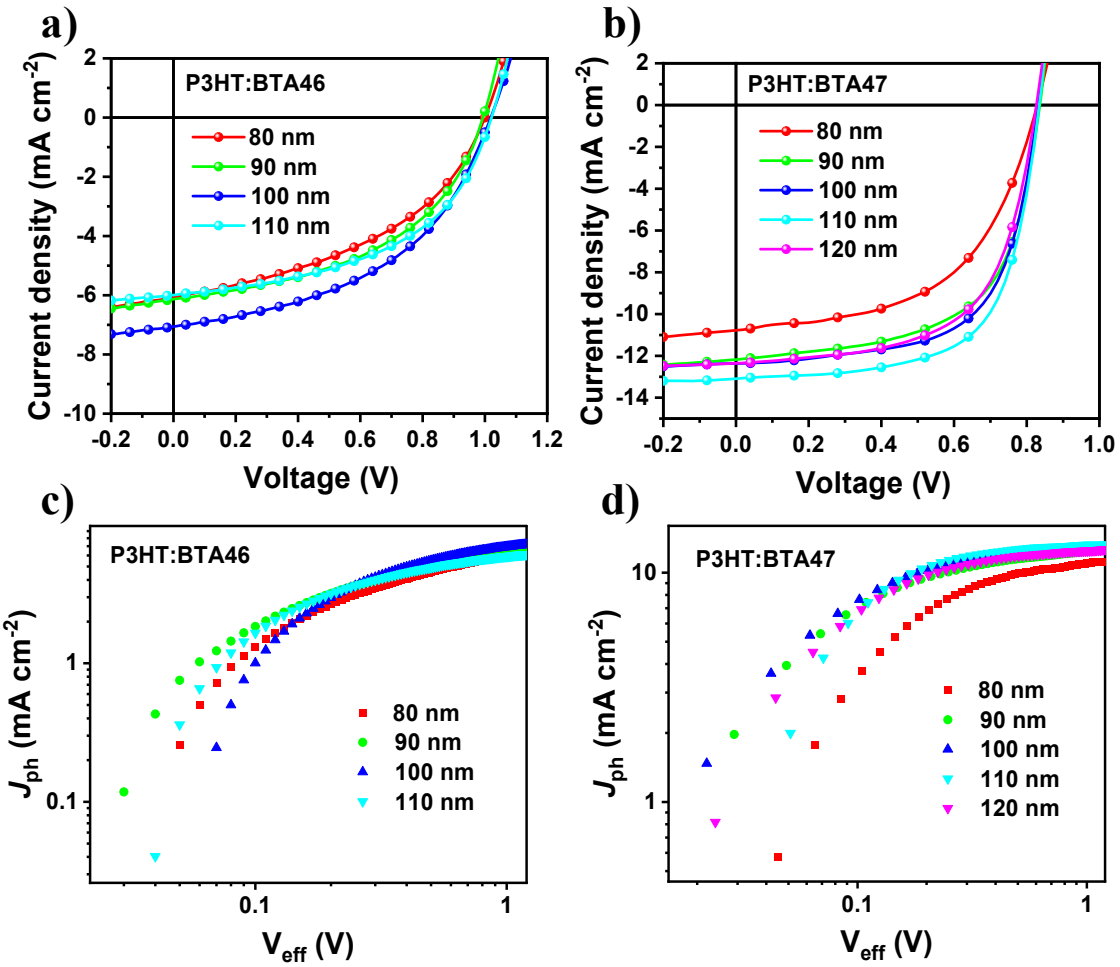

Figure S18. *J-V* and J_{ph}-V_{eff} images of different film thicknesses.

Table S1. D/A ratio optimization on the OSCs device performance. (ITO/PEDOT:PSS/active layer/Ca/Al).

Active layers	Solvent	D:A	V_{OC} (V)	J_{SC} (mA·cm^{-2})	FF	PCE (%)
P3HT:BTA46 (130 ℃)	CF	2:1	1.02	4.97	0.47	2.38
	CF	1.5:1	1.04	5.30	0.48	2.64
	CF	1:1	1.07	3.70	0.53	2.10
	CF	1:1.5	1.06	3.57	0.50	1.92
	CB	1.5:1	0.97	2.35	0.41	0.93
	DCB	1.5:1	0.74	1.58	0.33	0.39
P3HT:BTA47 (150 ℃)	CF	3:1	0.81	7.99	0.61	3.91
	CF	2:1	0.82	11.08	0.62	5.62
	CF	1.5:1	0.81	10.42	0.57	4.81
	CF	1:1	0.82	10.19	0.54	4.49
	CF	1:1.5	0.83	7.04	0.48	2.79
	CB	2:1	0.71	4.08	0.59	1.73
	DCB	2:1	0.81	1.35	0.51	0.56

Table S2. Influence of annealing temperature on device performance. (ITO/PEDOT:PSS/active layer/Ca/Al)

Active layers	Annealing (°C)	V_{OC} (V)	J_{SC} (mA·cm^{-2})	FF	PCE (%)
P3HT:BTA46 (1:1.5)	rt	1.03	4.07	0.35	1.47
	110	1.03	6.44	0.46	3.04
	120	1.02	6.58	0.45	2.99
	130	0.99	6.54	0.47	3.07
	140	1.00	5.71	0.50	2.87
	150	1.01	5.83	0.51	3.00
P3HT:BTA47 (2:1)	rt	0.84	5.70	0.32	1.53
	100	0.83	10.00	0.49	4.09
	130	0.83	11.27	0.50	4.66
	140	0.83	11.45	0.60	5.65
	150	0.83	11.46	0.62	5.86
	160	0.83	12.20	0.61	6.18
	170	0.81	12.03	0.53	5.16

Table S3. Influence of active layer concentration on device performance. (ITO/PEDOT:PSS/active layer/Ca/Al)

Active layers	Conc. ($mg \cdot mL^{-1}$)	Film thickness (nm)	V_{OC} (V)	J_{SC} ($mA \cdot cm^{-2}$)	FF	PCE (%)
P3HT:BTA46 (1:1.5, 130 ℃)	9	80	1.00	6.08	0.43	2.61
	12	90	0.99	6.13	0.44	2.67
	15	100	1.02	7.06	0.47	3.38
	18	110	1.02	5.99	0.49	3.00
P3HT:BTA47 (2:1, 160 ℃)	9	80	0.83	10.78	0.54	4.80
	12	90	0.84	12.18	0.61	6.18
	15	100	0.83	12.36	0.64	6.53
	18	110	0.83	13.09	0.65	7.12
	21	120	0.83	12.35	0.61	6.26

Table S4. Influence of additives on device performance. (ITO/PEDOT:PSS/active layer/Ca/Al)

Active layers	Additive	V_{OC} (V)	J_{SC} (mA·cm^{-2})	FF	PCE (%)
P3HT:BTA46 (1:1.5,130 ℃)	w/o	1.02	7.06	0.47	3.38
	6% Fc	1.03	7.25	0.53	3.99
	1% 1-CN	1.02	5.55	0.62	3.49
	1% DPE	1.01	5.74	0.62	3.62
	1% DIO	0.97	4.68	0.59	2.70
	1% DIM	0.00	0.00	0.00	0.00
P3HT:BTA47 (2:1, 160 ℃)	w/o	0.83	13.09	0.65	7.12
	6% Fc	0.84	11.92	0.58	5.76
	1% 1-CN	0.84	7.04	0.47	2.75
	1% DPE	0.84	7.64	0.59	3.74
	1% DIO	0.80	1.95	0.46	0.72
	1% DIM	0.82	3.37	0.41	1.15

Table S5. Influence of interface layer on device performance. (ITO/PEDOT:PSS/active layer/interface layer/Al)

Active layers	interface layer	V_{OC} (V)	J_{SC} (mA·cm^{-2})	FF	PCE (%)
P3HT:BTA46 (1:1.5,130 ℃)	Ca	1.03	7.25	0.53	3.99
	PFN-Br	1.01	7.10	0.49	3.51
	PDINO	0.99	5.87	0.47	2.73
P3HT:BTA47 (2:1, 160 ℃)	Ca	0.83	13.09	0.65	7.12
	PFN-Br	0.83	12.63	0.58	6.08
	PDINO	0.78	12.11	0.54	5.10

Table S6. Inverted devices performance. (ITO/ZnO/active layer/MoO_3/Al)

Active layers	V_{OC} (V)	J_{SC} (mA·cm^{-2})	FF	PCE (%)
P3HT:BTA46 (1:1.5,130 ℃)	1.02	7.06	0.47	3.37
P3HT:BTA47 (2:1, 160 ℃)	0.83	12.35	0.61	6.26

Table S7. Summary of decay time of P3HT, BTA46 and BTA47 neat films exciting at 450 nm and 650 nm, respectively.

Films	Probe (nm)	τ_1 (ps)	A1	τ_2 (ps)	A2	τ_3 (ps)	A3
P3HT	550	0.9±0.3	-40%	13±3.0	-39%	285±80	-21%
	1250	4.9±1.2	63%	89±9	37%		
BTA46	650	0.5±0.2	-51%	4.2±1.8	32%	71±25	-17%
	1150	0.8±0.1	47%	6.6±1.5	32%	57±9	21%
BTA47	680	0.9±0.2	-54%	10±3	-31%	142±46	-15%
	1130	0.7±0.1	49%	7.6±2.9	31%	53±10	20%

Table S8. In-plane (100) and out-of-plane (010) peaks, lamellar spacing (d) and π-π distance ($d_{\pi-\pi}$).

Blended films	Out of Plane		In Plane	
	(010)	*d*(Å) [a]	(100)	*d*(Å) [a]
P3HT:BTA46	1.667	3.77	0.346	18.16
P3HT:BTA47	1.655	3.80	0.351	17.90

[1] P N Murgatroyd. Theory of Space-Charge-Limited Current Enhanced by Frenkel Effect. *J. Phys. D Appl. Phys.* **1970,** 3 (2), 151-156